ELSEVIER

Gene Expression Patterns 7 (2007) 346–354

GEP

www.elsevier.com/locate/modgep

Tissue, cellular and sub-cellular localization of the Vangl2 protein during embryonic development: Effect of the *Lp* mutation

Elena Torban [a], Hui-Jun Wang [a], Anne-Marie Patenaude [a], Martin Riccomagno [c], Eugene Daniels [b], Douglas Epstein [c], P. Gros [a,*]

[a] *Department of Biochemistry, McGill University, 3655 Drummond, Room 907, Montreal, QC, Canada H3G-1Y6*
[b] *Department of Anatomy and Cell Biology, McGill University, Montreal, Canada*
[c] *Department of Genetics, University of Pennsylvania School of Medicine, Philadelphia, USA*

Received 5 April 2006; received in revised form 19 July 2006; accepted 21 July 2006
Available online 27 July 2006

Abstract

Loop-tail (*Lp*) mice show a very severe neural tube defect, craniorachischisis, which is caused by mis-sense mutations in the *Vangl2* gene. The membrane protein Vangl2 belongs to a highly conserved group of proteins that regulate planar polarity in certain epithelia, and that are also important for convergent extension movements during gastrulation and neurulation. A specific anti-Vangl2 antiserum was produced and used to examine the tissue, cell type, and sub-cellular localization of Vangl2 during embryogenesis. Vangl2 protein is expressed at high levels in the neural tube and shows a dynamic expression profile during neurulation. After neural tube closure, robust Vangl2 staining is detected in several neural and neurosensory tissues, including cerebral cortex, dorsal root ganglia, olfactory epithelium, retina, mechanosensory hair cells of the cochlea, and optic nerve. Vangl2 is also expressed during organogenesis in a number of tubular epithelia, including the bronchial tree, intestinal crypt/villus axis, and renal tubular segments derived from ureteric bud and from metanephric mesenchyme. Examination of Vangl2 localization in the neural tubes and cochleas of the normal and *Lp*/*Lp* embryos shows disruption of normal membrane localization of Vangl2 in independent alleles at *Lp* (*Lp*, Lp^{m1Jus}) as well as overall decrease in the expression level.

Keywords: Neural tube defetcs; Vangl2; Planar cell polarity; Looptail mouse model; Protein expression pattern; Tubulogenesis; Organogenesis; Neural tube closure

1. Results and discussion

Neural tube defects, NTDs, are amongst the most frequent and debilitating congenital abnormalities in humans, occurring in 1 per 1000 live births. The etiology of NTDs is complex and involves both genetic and environmental factors (Frey and Hauser, 2003). The molecular and cellular mechanisms regulating neural tube closure are extremely complex and poorly understood. However, the recent characterization of NTD mutants in vertebrates and invertebrates has identified genes, proteins and signaling pathways that are highly conserved during evolution and that play a critical role in neural tube formation. One such gene, *Vangl2*, is mutated in the mouse mutant *looptail* (*Lp*) (Kibar et al., 2001a; Kibar et al., 2001b; Murdoch et al., 2001). While *Lp*/+ heterozygotes show a characteristic kinked or "looped" tail, *Lp*/*Lp* homozygotes are not viable and display a very severe NTD (craniorachishisis) with failure of the neural tube to close from the midbrain-hindbrain region to the most caudal extremity of the embryo (Strong and Hollander, 1949).

Originally identified in *Drosophila* (*Van Gogh*/*Strabismus*) in a genetic screen for defects in planar cell polarity (Taylor et al., 1998; Wolff and Rubin, 1998), mammalian *Vangl2* belongs to the so-called core planar cell polarity (PCP) gene family (reviewed in Adler, 2002; Mlodzik, 2002). These genes are critical for establishment of planar

* Corresponding author. Tel.: +1 514 398 7291; fax: +1 514 398 2603.
E-mail address: philippe.gros@mcgill.ca (P. Gros).

1567-133X/$ - see front matter © 2006 Elsevier B.V. All rights reserved.
doi:10.1016/j.modgep.2006.07.007

(as opposed to basal-apical) polarity of cells within epithelial sheets (Gubb and Garcia-Bellido, 1982; Nübler-Jung et al., 1987). PCP is visible and has been best studied in the orientation of the eye unit structure (eight photoreceptor cells of the ommatidium) and the uniform polarity of hair (trichome) on wing cells. In vertebrates, PCP is noticeable in a number of structures, including the appearance of body hair, the uniform orientation of stereo-ciliary bundles on hair cells of the cochlea, and polarization of cilia in the oviduct (Guo et al., 2004; Montcouquiol et al., 2003; Chailley et al., 1987). In addition to Vangl2, the PCP family includes the plasma membrane receptor Frizzled (Fz), cytoplasmic proteins Dishevelled (Dsh/Dvl) and Prickle (Pk), and the atypical cadherins Flamingo (Fml) and Diego (Klingensmith et al., 1994; Theisen et al., 1994; Chae et al., 1999; Gubb et al., 1999; Usui et al., 1999; Feiguin et al., 2001; Jenny et al., 2005). During establishment of PCP in *Drosophila* wing epithelia, PCP proteins become asymmetrically re-distributed within each cell: the Vang-Pk complex assumes an apical–proximal position while Fz-Dsh accumulates at the apical–distal side (Axelrod, 2001; Tree et al., 2002; Bastock et al., 2003). The specific asymmetric localization of the PCP proteins appears to propagate a positional signal required for PCP (Fanto and McNeill, 2004).

Vertebrate orthologs of fly PCP genes have been cloned (Kibar et al., 2001a; Park and Moon, 2002; Carreira-Barbosa et al., 2003; Goto and Keller, 2002; Wallingford et al., 2000; Curtin et al., 2003; Hamblet et al., 2002; Wang et al., 2006a) and have been shown to regulate convergent extension (CE) movements in zebrafish and *Xenopus* embryos (Wallingford and Harland, 2002; Torban et al., 2004a). During gastrulation, dorsal mesenchymal cells and neuroepithelial cells polarize by forming medial–lateral protrusions, which enable cells to move specifically toward the midline; cells interdigitate with each other, causing lengthening of the tissues in the anterior–posterior direction with concomitant thinning in the medial–lateral direction. CE contributes significantly to neural tube closure and is regulated by a vertebrate counterpart of fly PCP signaling referred to as the non-canonical Wnt pathway (Fanto and McNeill, 2004). Similar to *Lp* mice, homozygous mutants of *Celsr1* (mammalian ortholog of *Flamingo*) (Curtin et al., 2003) and double *Fz3*/*Fz6* or *Dvl1*/*Dvl2* mutants (Wang et al., 2006a; Hamblet et al., 2002) exhibit craniorachischisis. Alterations in the organization of ciliary bundles of cochlear hair cells are also detected in each of these mutants (Curtin et al., 2003; Wang et al., 2006a; Wang et al., 2006b).

Although an open neural tube (craniorachischisis) and cochlea disorganization are the most evident defects in *Lp* mice, a number of additional developmental abnormalities have been noted, including defects in the heart (Henderson et al., 2001), alterations in optic nerve trajectories (Rachel et al., 2000), minor cerebral abnormalities (Wilson, 1982; Kibar et al., 2001b), open eyelids and malfunction of the reproductive system (Strong and Hollander, 1949). mRNA expression studies have previously detected *Vangl2* mRNA in the neural tube (Kibar et al., 2001a; Tissir and Goffinet, 2006). However a detailed analysis of the cellular and subcellular distribution of the Vangl2 protein in embryonic tissues has yet to be reported. In this report, we investigated the expression of Vangl2 protein in developing mouse embryos. This was carried out to identify tissues and cell types in which the protein may play a role in PCP or CE, and that may be disrupted by the *Lp* mutation. To understand the mechanisms contributing to developmental defects seen in *Lp* mice, we compared Vangl2 protein distribution in neural tube and cochlea of normal mice and of both known alleles at the *Looptail* mutation (*Lp* and Lp^{m1Jus}).

1.1. Detection of Vangl2 protein by immunoblotting

To study Vangl2 expression *in vivo*, we raised polyclonal rabbit antisera against a fusion protein consisting of the predicted N-terminal cytoplasmic portion of the Vangl2 (13–64 amino acids) fused in-frame to GST. This segment was chosen because it is not conserved in Vangl1 (~40% similarity), the second Van Gogh-like gene, and yields specific antiserum when used as immunogen (Torban et al., 2004b). Immunoblotting experiments with this antiserum using mouse tissues from E13.5 embryos (Fig. 1A) shows the presence of a single band of the expected ~65 kDa size in the head (lane 2) but not in the trunk of the same embryo (lane 1). Its electrophoretic mobility is similar to that of Vangl2 protein expressed in HEK293 cells transfected with full-length *Vangl2* cDNA and used as a positive control (Fig. 1A, lane 5). Neither neocortex nor striatum from adult mice had detectable levels of Vangl2 protein (Fig. 1A, lanes 3 and 4). The Vangl2 protein was enriched in membrane fractions (Fig. 1B, lanes 1 and 3) compared to total cell lysates (Fig. 1B, lanes 2 and 4).

1.2. Vangl2 expression in developing neural tube

Craniorachischisis is the most noticeable defect in the *Lp* mouse. Apparently, it arises from a failure of neuroepithelial cells to undergo convergent extension and, perhaps, as

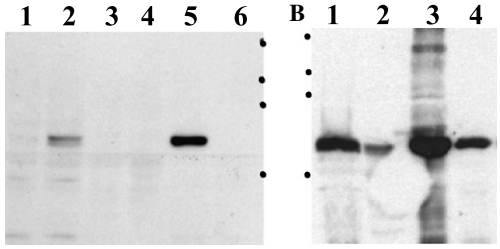

Fig. 1. Detection of Vangl2 protein in mouse embryonic and adult tissues. (A) Expression of Vangl2 in fetal tissues: lane 1, E13.5 trunk; lane 2, E13.5 head; lane 3, adult cortex; lane 4, adult striatum; lane5, HEK293 cells expressing a transfected *Vangl2* cDNA construct used as positive control; lane 6, HEK293 cells transfected with control pCB6 vector. (B) Vangl2 protein is enriched in membrane fractions: lane1, membrane fraction from E13.5 fetal brain; lane2, total E13.5 fetal brain lysate; lane3, membrane fraction from *Vangl2* transfected HEK293 cells; lane 4, whole cell lysate of the *Vangl2* transfected HEK293 cells.

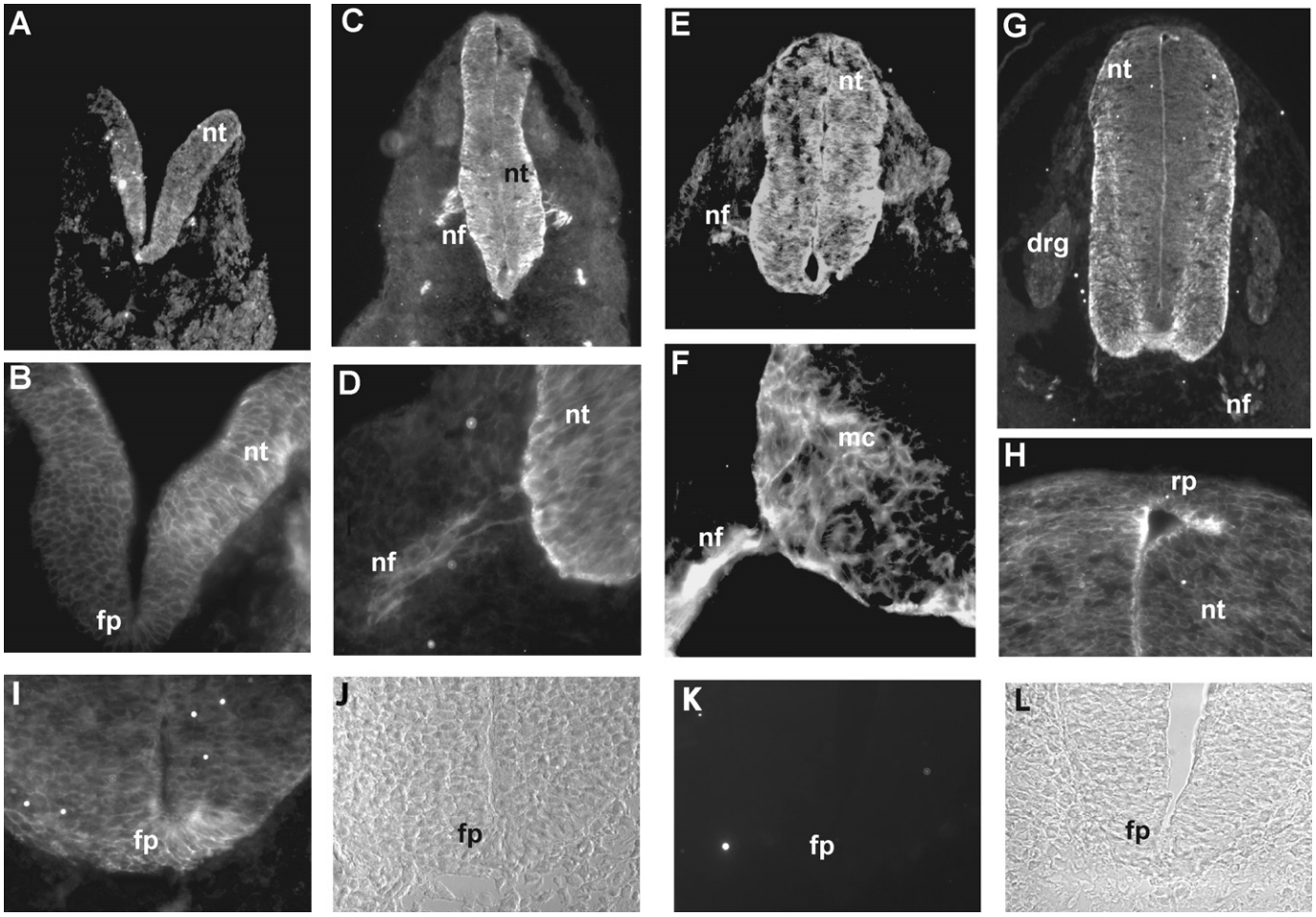

Fig. 2. Vangl2 protein expression in the developing neural tube. (A) Transverse section of E7.5 embryo, ×200. (B) NT view of the E7.5 embryo, ×630. (C) Transverse section of E9.0 embryo at the forelimb level, ×200. (D) Magnified view of the neural tube and the forming spinal nerves at E9.0, ×630. (E) Transverse section of E10.5, ×200. (F) Ventro-lateral view of the NT and the spinal nerve at E10.5, ×630. (G) Transverse section of the E11.5 embryo, ×100. (H) Magnified view of the roof plate of the section in (G), ×630. (I) E10.5 NT section at the heart level stained with for Vangl2, ×630. (J) Light microscopy image of (I), ×630. (K) E10.5 NT floor plate section stained with pre-immune serum, ×630. (L) Light microscopy image of section in (K). *Abbreviations: drg*, dorsal root ganglia; *fp*, floor plate; *mc*, motor column; *nf*, neural fibers; *nt*, neural tube; *rp*, roof plate.

recently reported, from their inability to establish the proper orientation of mitotic spindles during cell divisions, which, in turn, affects directional cell movements (Gong et al., 2004). Therefore, we investigated Vangl2 protein expression in the NT prior to, during and after closure (E7.5–E11.5). At E7.5, we detected Vangl2 protein in the neuroepithelium of the entire NT (Fig. 2A). Examination of the NT sections under higher magnification showed clear membrane-associated staining of Vangl2 protein (Fig. 2B). No other Vangl2-positive sites were detected. At E8.5–9, Vangl2 protein was found highly expressed throughout the NT (Fig. 2C). However, in the posterior region, where the NT is not yet fully closed, Vangl2 expression appeared stronger than in the more rostral closed part. In addition, neural fibers sprouting from the NT were positive for Vangl2 expression (Figs. 2C and D). Low Vangl2 protein presence was detected in the epithelial lining of the foregut and midgut (data not shown).

At E10.5, Vangl2 protein was detected in all cells of the closed NT including the floor plate (Fig. E, F, I, J). Lower levels of Vangl2 protein were detected in dorsal root ganglia (DRG) and in non-neuronal tissues including the mesonephric and major bronchial ducts as well as in the most distal part of the forelimb bud and in the ectoderm (data not shown). We did not detect high background staining in the sections exposed only to the pre-immune serum (Fig. 2K and L).

At E11.5, Vangl2 was still mostly confined to the neural epithelium but its expression level was lower than at earlier developmental stages (Fig. 2H). Within the NT, Vangl2 protein was redistributed more radially toward the mantle zone (Fig. 2H). In the ventral NT, Vangl2 was detected in the motor columns and in the axons of the commissural neurons as well as in the outgrowing motor and sensory neuronal fibers (Fig. 2G). We also observed Vangl2 protein in the epithelium of the esophagus, trachea, major bronchi, mesonephric ducts and tubules (not shown). Therefore, the pattern of Vangl2 protein expression in the developing NT parallels that of Vangl2 mRNA and is similar to the patterns reported for other PCP genes, including Celsr1-3, Prickle1-2, and

PTK7 (Bekman and Henrique, 2002; Lu et al., 2004; Shima et al., 2002; Tissir and Goffinet, 2006).

1.3. Vangl2 expression in CNS at E16.5

At E16.5, robust Vangl2 protein expression was detected in the intermediate and outer marginal zones of cerebral cortex, with a lower level in the mantle zone and no expression in the ventricular layer (Fig. 3A). Cranial ganglia were also positive for Vangl2, including the facial ganglion and its rootlets (Fig. 3D) and the trigeminal ganglion (Fig. 3I and J). In these structures, Vangl2 expression level appears equally high in the soma and in the neural fibers. In zebrafish Vangl2 mutant *trilobite*, a specific abnormality of the tangential relocation of branchiomotor neurons (which correspond to the facial neuronal ganglia VII) has been detected (Jessen et al., 2002). Particularly high Vangl2 protein expression was noted in the facial ganglia.

At E16.5, DRGs were positive for Vangl2 (Fig. 3E), and in the ventral spinal cord, high level of the protein was observed in motor neuron columns (Fig. 3C). We detected strong Vangl2 protein expression in the olfactory

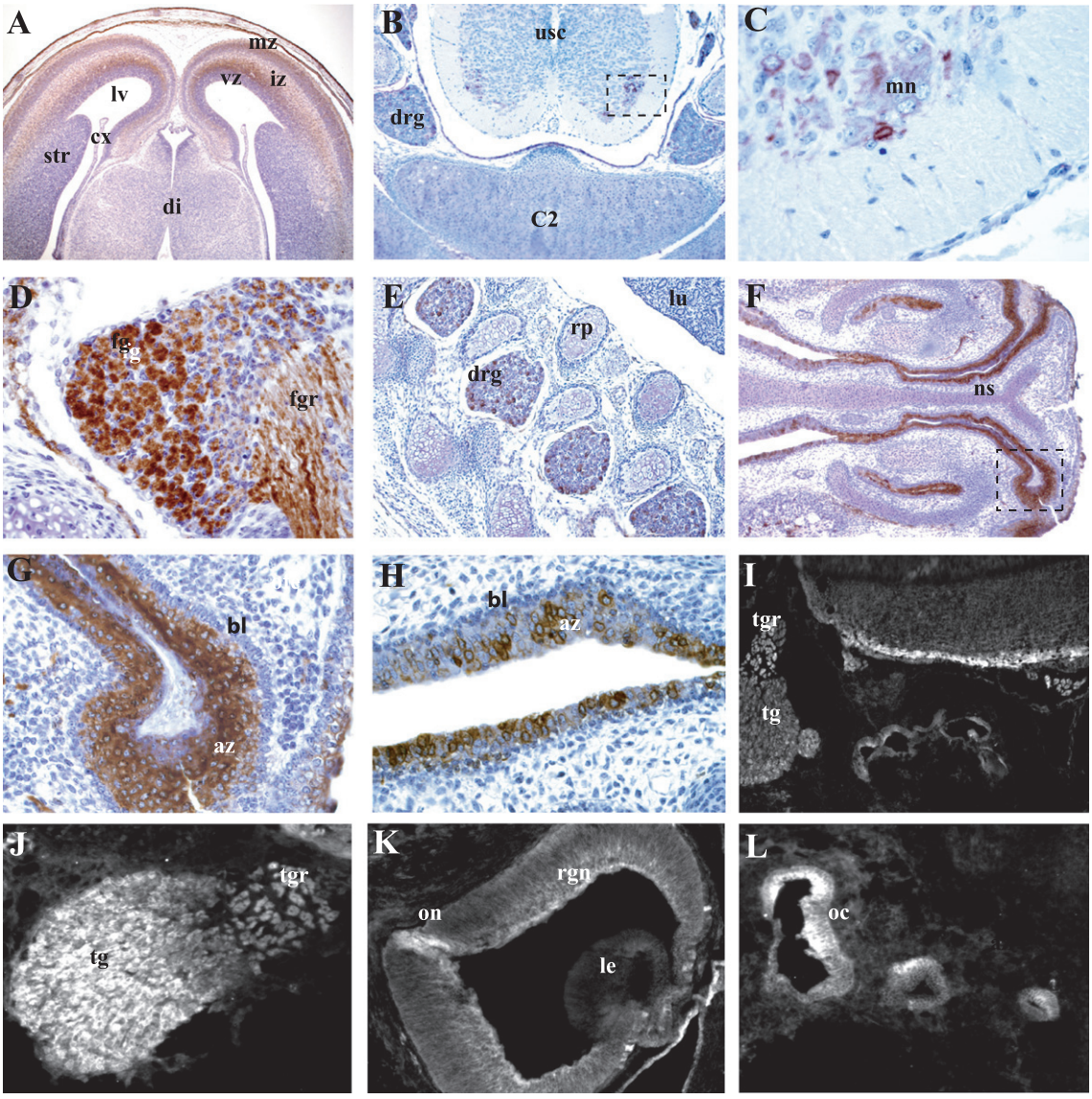

Fig. 3. Vangl2 protein expression in the neuroepithelium-derived tissues and structures. All sections are from E16.5. (A) Section from the crown part of the coronal brain, ×200. (B) Transverse section at the level of the C2 vertebra, ×200. (C) Part of the ventral horn of the spinal cord containing motor neurons (×600) identified by a rectangle in (B). (D) Facial ganglion and its rootlets, ×600. (E) Sagital section through dorsal root ganglia, ×200. (F) Transverse section at the level of nasal cavity, ×200. (G) Magnified view of the olfactory epithelium at the front of nasal cavity, ×600. (H) Olfactory epithelium in the dorsal part of the nasal cavity, ×400. (I) Transverse section through trigeminal ganglion and inner ear, ×100. (J) Trigeminal ganglion and its rootlets, ×200. (K) Transverse section of the eye and optic nerve, ×200. (L) Transverse section through inner ear, including the organ of Corti, ×200. *Abbreviations: az*, apical zone; *bl*, basal layer; *cx*, choroids plexus; *di*, diencephalons; *drg*, dorsal root ganglia; *fg*, facial ganglion; *fgr*, facial ganglion rootlets; *iz*, intermediate zone; *le*, lens; *lu*, lungs; *lv*, lateral vesicle; *mn*, motor neurons; *mz*, mantal zone; *ns*, nasal cavity; *oc*, organ of Corti; *on*, optic nerve; *rgn*, retinal ganglionic neurons; *rp*, rib primordium; *str*, striatum; *tg*, trigeminal ganglion; *trg*, trigeminal ganglion rootlets; *usc*, upper spinal cord; *vz*, ventricular zone.

epithelium (Figs. 3F–H). In the ventral (frontal) part of the nasal cavity, the majority of the cells of the apical and middle layers (but not the basal layer) appeared to be Vangl2 immunoreactive (Fig. 3G). The basal layer is populated with progenitor cells whereas the middle and apical layers are enriched for premature and differentiated neurons, respectively. In more dorsal and dorso-lateral portions of the nasal cavity, we observed membrane-associated Vangl2 in fewer cells, predominantly in the apical zone (Fig. 3H). Vangl2 protein was also detected throughout the retina (Fig. 3K). By E16.5, the retina has differentiated into outer (ONL) and inner (INL) neuronal layers, including precursors of the ganglion cells in the latter. Retinal ganglion neurons sprout axons which bundle up to form an optic nerve. *Lp* and another mouse mutant with craniorachischisis, *circletail* (which harbors a mutation in *Scribble1* gene), display axonal tract abnormalities of the optic nerve (Rachel et al., 2000; Murdoch et al., 2003). We found high Vangl2 expression in the INL layer, particularly in the precursors of retinal ganglion cells and in the optic nerve.

High Vangl2 expression was also detected in the neurosensory epithelium of various structures of the inner ear (Fig. 3I and L); particularly high expression was observed in the organ of Corti (Fig. 3L). Vangl2 staining was clearly membrane-associated in cells from the retina, olfactory epithelium, and of the cochlea, (Fig. 3H, K, and L).

1.4. Vangl2 expression during organogenesis in late-gestation

By E16.5, Vangl2 protein was found in several organs, but was restricted to discrete cell populations. Strong Vangl2 expression was detected in the outer layer of the cornea (Fig. 4A and B) and in the outer eyelid epithelium (Fig. 4B), both derivatives of the surface ectoderm. In younger E15.5 embryos, we detected Vangl2 at the site of eyelid fusion (not shown). In *Lp* and other PCP mouse mutants (e.g., *Circletail* and *Fz3;Fr6* double homozygotes) eyelids remain open. Vangl2 was found in the skin epidermis (Fig. 4I and J) and in the shafts of the hair and whisker follicles (Fig. 4I and J).

Vangl2 protein was observed in a number of epithelia from glandular and tubular structures. It was evident in various compartments of the gastrointestinal epithelium (Fig. 4C and D), respiratory epithelium of the main and terminal bronchi (Fig. 4E and F), and in both lineages contributing to metanephric kidney, ureteric bud and condensing mesenchyme (Fig. 4G and H). We also detected Vangl2 protein in the esophagus (Fig. 4K) and in epithelia of salivary glands and trachea (not shown). Vangl2 protein was localized to the cell membrane in esophagus (Fig. 4K), kidney (Fig. 4H), lung (Fig. 4F), epidermis and hair follicles (Fig. 4J). In all cases, Vangl2 protein expression was robust, membrane associated and, in most cases, seemingly restricted to the basolateral or lateral aspects of epithelial cells (Fig. 4J and K). Many of these structures are polarized and undergo convergent extension as they elongate and grow directionally (e.g., bronchial and mesonephric ducts). Recently, Fischer et al. reported that the PCP pathway is implicated in longitudinal tubular growth by establishing proper mitotic alignment of proliferating tubular cells (Fischer et al., 2006). It also was shown that inversin, a kidney protein mutated in human patients with inherited nephronophthisis, interferes with CE movements and physically interacts with Dvl and Vangl2, thereby switching off the canonical Wnt pathways and causing partial Dvl degradation (Simons et al., 2005). Interestingly, Vangl2 was detected in the ciliary basal body in cultured kidney collecting duct cells (Ross et al., 2005).

1.5. Sub-cellular localization of Vangl2 in neural tube of wild type and Lp−/− embryos

In *Looptail* mice, neural tube is not formed properly. Therefore, we examined Vangl2 protein expression pattern in NT of the E10.5 wild type embryos and in both allelic variants of the *Lp* mutation (S464N and D255E). As seen in Fig. 5, strong Vangl2 immunoreactivity was detected in the wildtype neuroepithelial cells (Figs. 5 A–C;); Vangl2 protein was detected mostly at the cell membrane and at the lower level in intracellular endomembrane compartments (Fig. 5A and inset). In these cells, Vangl2 staining was found to overlap with that produced by β-catenin, which is detected primarily at the plasma membrane in association with E-cadherin (Kemler, 1993) (Fig. 5B and inset). The merged image (Fig. 5C and inset) confirms substantial co-localization of Vangl2 and β-catenin at the cell membrane. Examination of the NT tissues from the *Lp*/*Lp* mouse revealed a dramatic difference in the expression pattern of the mutant protein. The mutant Vangl2^{D255E} protein variant appeared to have lost its membrane localization (Fig. 5D and F), with all staining restricted to intracellular compartments. This staining was clearly distinct from that of β-catenin with little overlap detected in the merged images (Fig. 5F). The level of Vangl2^{D255E} protein also appeared reduced.

In addition to the severe NT defect, *Lp* mice have been shown to have a specific distortion of planar polarity of the stereociliary bundles in cochlear hair cells. We examined Vangl2 protein expression in the organ of Corti of wildtype and *Lp*/*Lp* embryos from both mutant stocks (Supplementary material). In wildtype tissues, Vangl2 protein could be readily visualized in association with the plasma membrane of the hair cells (Supplementary material, panels A, B, E, G; S464N variant is shown). In the mutant cochlea, we detected a loss of the membrane-associated Vangl2 staining similar to that seen in the NT while β-catenin was still detected at the plasma membrane (Supplementary material, panels F, H, J, L). The cytoplasmic level of the mutant protein was moderately decreased.

Vangl2 has been shown to bind Dvl and Pk and to bring about their translocation to the cell membrane, assuring proper sub-cellular compartmentalization of these PCP proteins and, possibly, anchoring the PCP protein complex (Park and Moon, 2002; Bastock et al., 2003). We have recently reported that the D255E and S464N mutations (*Lp*) impair the ability of the cytoplasmic domain of Vangl2

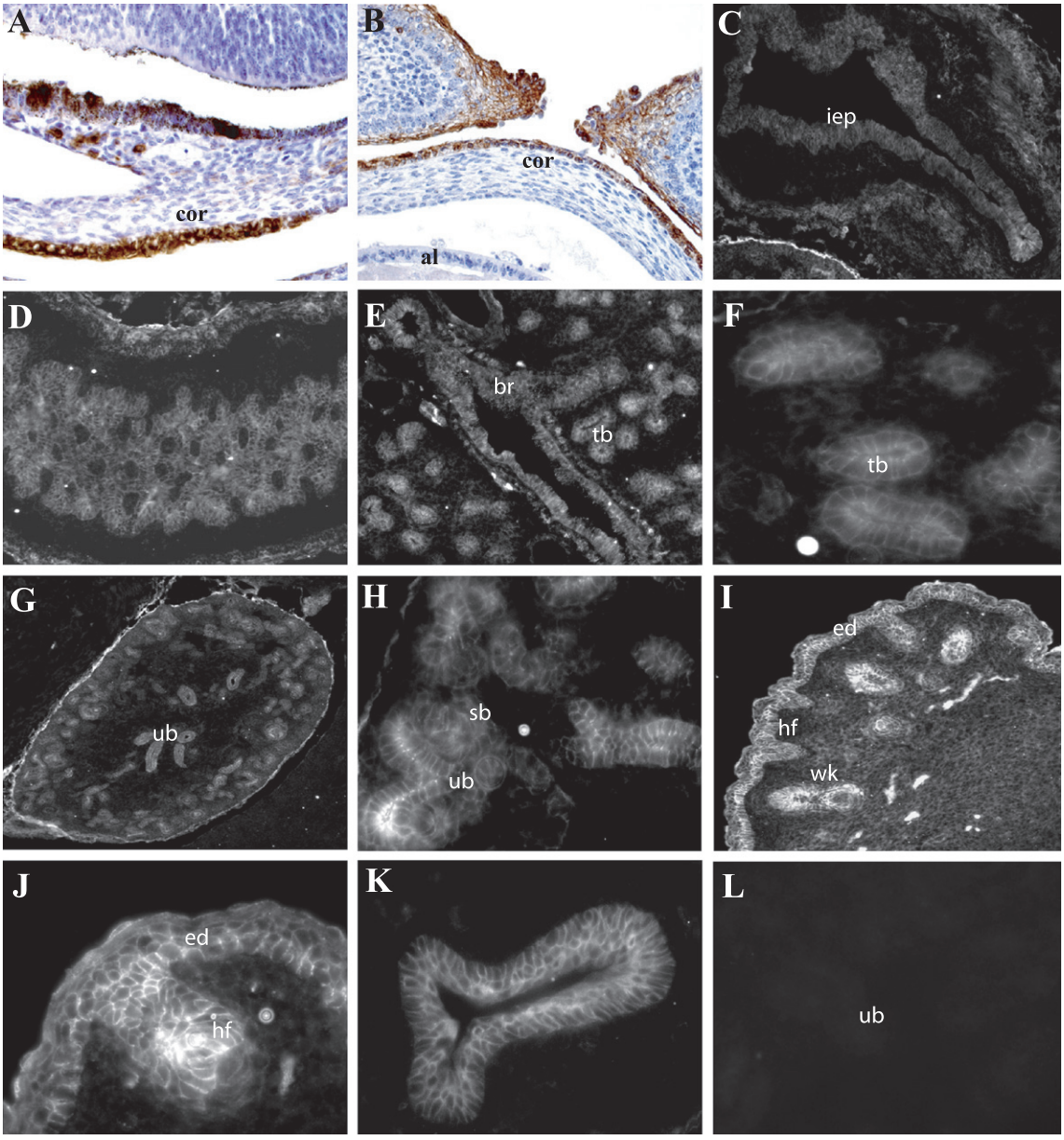

Fig. 4. Vangl2 protein expression during organogenesis. All sections are from E16.5. (A) Transverse section through the iris of the eye, ×600. (B) Transverse section through the closing eye lid, ×600. (C) Stomach, ×200. (D) Sagital section through duodenum, ×200. (E) Lung, ×100. (F) Magnified view of the respiratory epithelium of the terminal bronchi, showing basolateral Vangl2 staining, ×630. (G) Kidney, ×100. (H) Tips of the ureteric bud and the condensing mesenchyme in the kidney, ×200. (I) Transverse section through the upper jaw with shafts of hair and whisker follicles positive for Vangl2 protein, ×100. (J) Skin fragment of the trunk, ×630. (K) Esophagus, ×630. (L) Kidney section stained with pre-immune serum and used as negative control, ×200. *Abbreviations: al*, anterior lens; *br*, main bronchi; *cor*, cornea; *ed*, epidermis; *hf*, hair follicle; *iep*, interstitial epithelium; *stm*, smooth muscle cells; sb, S-shaped body in the kidney; *tb*, terminal bronchi; *ub*, ureteric bud; *wk*, whisker follicle.

to physically interact with Dvl proteins (Torban et al., 2004b). Here, we further report that both *Lp*-specific mutant Vangl2 variants have altered sub-cellular distributions and a decreased expression level.

Experimental procedures

1.6. Preparation of embryos

Embryos from CD-1 mice (Charles River) were collected at various developmental stages. Embryos from *Looptail* mice (*Lp* and Lp^{m1Jus}) were harvested at E9.5, E10.5, E14.5 and E16.5 and phenotyped for presence of NTD or looped tail by visual inspection. For immunohistochemistry experiments, embryos were fixed in Bouin's solution, dehydrated in increasing concentrations of ethanol, embedded in paraffin and sectioned. For immunofluorescence, embryos were fixed in 4% paraformaldehyde, washed in phosphate buffered saline (PBS) and cryo-preserved with an OCT embedding compound.

1.7. Immunohistochemistry

The production of the polyclonal rabbit anti-Vangl2 antiserum has been previously described (Torban et al., 2004b). Eight μm paraffin-embedded

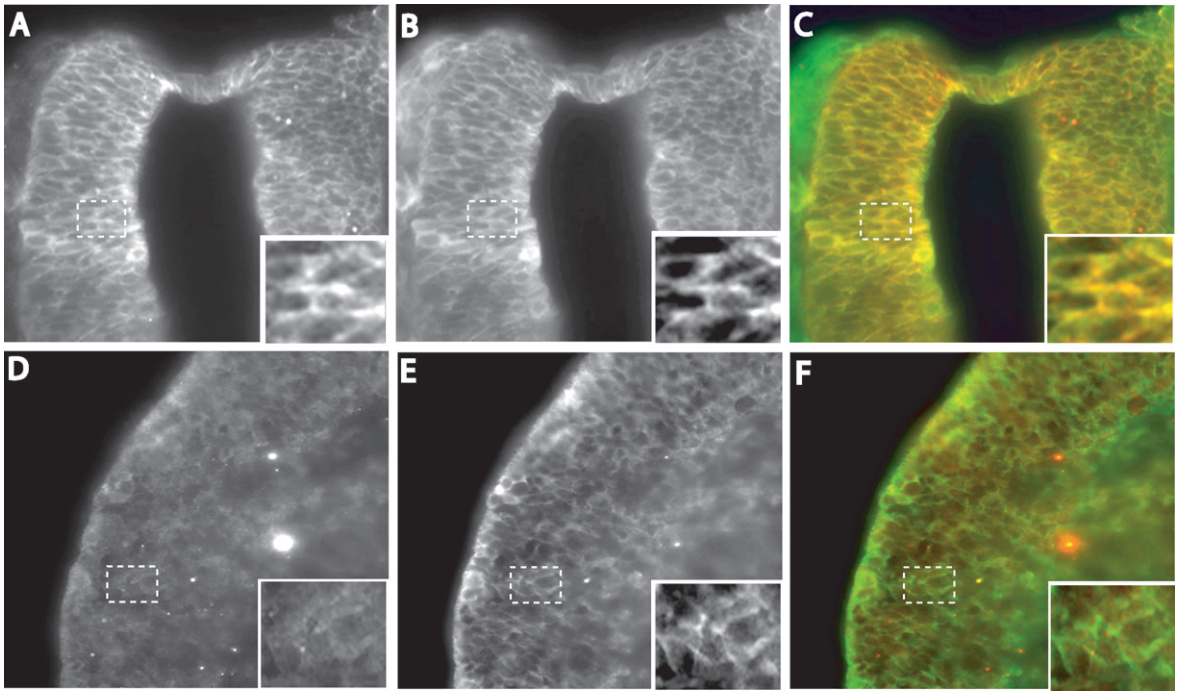

Fig. 5. Localization of the Vangl2 protein in the neuroepithelium of normal and of *Lp* emrbyos. (A) Vangl2 protein is abundant and membrane-associated in the neuroepithelium of the neural tube of the wildtype E10.5 embryos, ×630, inset ×1800. (B) The same section as in (A), stained with an anti-β-catenin monoclonal antibody that detects membrane-associated β-catenin expression, ×630, inset ×1800. (C) Merged image of (A) and (B), Vangl2 red, β-catenin green, ×630, inset ×1800. (D) Vangl2 protein is detected in the open neural tube of the matching *Lp*/*Lp* embryos, however, its concentration is reduced and cell membrane-association is apparently lost, ×630, inset ×1800. (E) The same section as in (D), stained with anti-β-catenin antibody, ×630, inset ×1800. (F) Merged image of (D) and (E), arrows specify exclusively β-catenin membrane staining (green) and a loss of the Vangl2 protein (red) at the plasma membrane, ×630, inset ×1800.

sections were prepared, hydrated, incubated overnight with either anti-Vangl2 rabbit sera or pre-immune serum as a negative control. Briefly, sections were treated with 1.5% hydrogen peroxidase, blocked in biotin-avidin solution (DAKO) followed by blocking in 10% normal goat serum for 30 min and incubation overnight with polyclonal Vangl2 antibody (1:500 dilution). All washes were done in TBST (0.15 M NaCl, 0.01 M Tris–HCl, pH 7.4, 0.05% Tween 20), sections were counterstained with Harris' hematoxylin and mounted with Permount. Visualization was carried out using a commercially available kit (CSA DAKO K1500; DAKO Cytomation) exactly according to the manufacturer's recommendations.

Twelve to sixteen μm cryosections were fixed in 4% PFA, boiled for 6 min in 10 mM citric buffer, pH 6.0, blocked in a solution containing 10% normal goat serum, 0.4% Triton for 1 h and incubated with anti-mouse Vangl2 polyclonal rabbit antibody (1:75 dilution) overnight. The Vangl2 immuno-complexes were revealed by incubation with Cy3-conjugated goat anti-rabbit antibody (Jakson ImmunoResearch). Monoclonal anti-mouse β-catenin antibody was used (1:500). Sections were analyzed and photographed with a Zeiss microscope using the Axio Vision 4.3 software package (Carl Ziess Vision GmbH).

1.8. Cell culture and transfections

Human embryonic kidney 293 cells were cultured in DMEM medium supplemented with 10% fetal bovine serum and streptomycin and penicillin (Gibco). Cells were seeded in 100 mm tissue culture dishes 20 h prior to transfection with 2 μg of the pCMV-mVangl2-myc expression vector (described in Torban et al., 2004b) using Lipofectamine 2000, as described by the manufacturer (Invitrogen). Cells were harvested 24 h post-transfection, washed in PBS and lysed in a buffer containing 50 mM Tris, pH 7.4, 10% glycerol, 150 mM NaCl, 1% Triton, 1 mM PMSF, 10 μg/ml leupeptin and aprotonin. Crude membrane fractions were prepared by ultracentrifugation. Total brain lysates and crude brain membrane fractions were prepared from mouse E13.5 brain and adult tissues using a similar protocol. Proteins (50 μg per lane) were resolved by SDS/PAGE and transferred to a nitrocellulose membrane; immunodetection was carried out with anti-Vangl2 antibody (1:500 dilution) and HPR-conjugated anti-rabbit secondary antibody (Jackson ImmunoResearch).

Acknowledgements

The authors are indebted to Susan Gauthier for maintenance of the *Lp* mouse colony. This work was supported by a grant to PG from the Canadian Institutes of Health Research (CIHR). PG is supported by a Distinguished Scientist salary award from CIHR and is a James McGill Professor of Biochemistry. ET is supported by a post-doctoral fellowship from the CIHR.

Appendix A. Supplementary data

Supplementary data associated with this article can be found, in the online version, at doi:10.1016/j.modgep.2006.07.007.

References

Adler, P.N., 2002. Planar signaling and morphogenesis in *Drosophila*. Developmental Cell 2, 525–535.

Axelrod, J.D., 2001. Unipolar membrane association of Dishevelled mediates Frizzled planar cell polarity signaling. Genes and Development 15, 1182–1187.

Bastock, R., Strutt, H., Strutt, D., 2003. Strabismus is asymmetrically localized and binds to Prickle and Dishevelled during *Drosophila* planar polarity patterning. Development 130, 3007–3014.

Bekman, E., Henrique, D., 2002. Embryonic expression of three mouse genes with homology to the *Drosophila melanogaster* prickle gene. Mechanisms of Development 119 (Suppl 1), S77–S81.

Carreira-Barbosa, F., Concha, M.L., Takeuchi, M., Ueno, N., Wilson, S.W., Tada, M., 2003. Prickle 1 regulates cell movements during gastrulation and neuronal migration in zebrafish. Development 130, 4037–4046.

Chae, J., Kim, M.J., Goo, J.H., Collier, S., Gubb, D., Charlton, J., Adler, P.N., Park, W.J., 1999. The *Drosophila* tissue polarity gene starry night encodes a member of the protocadherin family. Development 126, 5421–5429.

Chailley, B., Nicolas, G., Laine, M.C., 1987. Organization of actin microfilaments in the apical border of oviduct ciliated cells. Biol Cell 67 (1), 81–90.

Curtin, J.A., Quint, E., Tsipouri, V., Arkell, R.M., Cattanach, B., Copp, A.J., Henderson, D.J., Steel, N., Brown, S.D.M., Gray, I.C., Murdoch, J.N., 2003. Mutation of *Celsr1* disrupts planar polarity of inner ear hair cells and causes severe neural tube defects in the mouse. Current Biology 13, 1129–1133.

Fanto, M., McNeill, H., 2004. Planar polarity from flies to vertebrates. Journal of Cell Science 117 (Pt 4), 527–533.

Feiguin, F., Hannus, M., Mlodzik, M., Eaton, S., 2001. The ankyrin repeat protein Diego mediates Frizzled-dependent planar polarization. Development Cell 1, 93–101.

Fischer, E., Legue, E., Doyen, A., Nato, F., Nicolas, J.F., Torres, V., Yaniv, M., Pontoglio, M., 2006. Defective planar cell polarity in polycystic kidney disease. Nature Genetics 38 (1), 21–23.

Frey, L., Hauser, W.A., 2003. Epidemiology of neural tube defects. Epilepsia 44 (Suppl. 3), 4–13.

Goto, T., Keller, R., 2002. The planar cell polarity gene strabismus regulates convergence and extension and neural fold closure in *Xenopus*. Developmental Biology 247 (1), 165–181.

Gong, Y., Mo, C., Fraser, S.E., 2004. Planar cell polarity signalling controls cell division orientation during zebrafish gastrulation. Nature 430, 689–693.

Gubb, D., Garcia-Bellido, A., 1982. A genetic analysis of the determination of cuticular polarity during development in *Drosophila melanogaster*. Journal of embryology and Experimental Morphology 68, 37–57.

Gubb, D., Green, C., Huen, D., Coulson, D., Johnson, G., Tree, D., Collier, S., Roote, J., 1999. The balance between isoforms of the prickle LIM domain protein is critical for planar polarity in *Drosophila* imaginal discs. Genes and Development 13, 2315–2327.

Guo, N., Hawkins, C., Nathans, J., 2004. Frizzled6 controls hair patterning in mice. Proceedings of the National Academy of Sciences, USA 101 (25), 9277–9281.

Hamblet, N.S., Lijam, N., Ruiz-Lozano, P., Wang, J., Yang, Y., Luo, Z., Mei, L., Chien, K.R., Sussman, D.J., Wynshaw-Boris, A., 2002. Dishevelled 2 is essential for cardiac outflow tract development, somite segmentation and neural tube closure. Development 129, 5827–5838.

Henderson, D.J., Conway, S.J., Greene, N.D., Gerrelli, D., Murdoch, J.N., Anderson, R.H., Copp, A.J., 2001. Cardiovascular defects associated with abnormalities in midline development in the Loop-tail mouse mutant. Circulation Research 89 (1), 6–12.

Jenny, A., Reynolds-Kenneally, J., Das, G., Burnett, M., Mlodzik, M., 2005. Diego and Prickle regulate Frizzled planar cell polarity signalling by competing for Dishevelled binding. Nature Cell Biology 7, 691–697.

Jessen, J.R., Topczewski, J., Bingham, S., Sepich, D.S., Marlow, F., Chandrasekhar, A., Solnica-Krezel, L., 2002. Zebrafish *trilobite* identifies new roles for Strabismus in gastrulation and neuronal movements. Nature Cell Biology 4, 610–615.

Kemler, R., 1993. From cadherins to catenins: cytoplasmic protein interactions and regulation of cell adhesion. Trends in Geneics 9, 317–321.

Kibar, Z., Underhill, D.A., Canonne-Hergaux, F., Gauthier, S., Justice, M.J., Gros, P., 2001b. Identification of a new chemically induced allele (Lp(m1Jus)) at the loop-tail locus: morphology, histology, and genetic mapping. Genomics 72, 331–337.

Kibar, Z., Vogan, K.J., Groulx, N., Justice, M.J., Underhill, D.A., Gros, P., 2001a. Ltap, a mammalian homolog of *Drosophila Strabismus*/*Van Gogh*, is altered in the mouse neural tube mutant Looptail. Nature Genetics 28, 251–255.

Klingensmith, J., Nusse, R., Perrimon, N., 1994. The *Drosophila* segment polarity gene dishevelled encodes a novel protein required for response to the wingless signal. Genes and Development 8, 118–130.

Lu, X., Borchers, A.G., Jolicoeur, C., Rayburn, H., Baker, J.C., Tessier-Lavigne, M., 2004. PTK7/CCK-4 is a novel regulator of planar cell polarity in vertebrates. Nature 430, 93–98.

Mlodzik, M., 2002. Planar cell polarization: do the same mechanisms regulate Drosophila tissue polarity and vertebrate gastrulation? Trends in Genetics 18, 564–571.

Montcouquiol, M., Rachel, R.A., Lanford, P.J., Copeland, N.G., Jenkins, N.A., Kelley, M.W., 2003. Identification of *Vangl2* and *Scrb1* as planar polarity genes in mammals. Nature 423, 173–177.

Murdoch, J.N., Henderson, D.J., Doudney, K., Gaston-Massuet, C., Phillips, H.M., Paternotte, C., Arkell, R., Stanier, P., Copp, A.J., 2003. Disruption of scribble (*Scrb1*) causes severe neural tube defects in the circletail mouse. Human Molecular Geneics 12, 87–98.

Murdoch, J.N., Doudney, K., Patemotte, C., Copp, A.J., Stanier, P., 2001. Severe neural tube defects in the loop-tail mouse result from mutation of Lppl, a novel gene involved in floor plate specification. Human Molecular Genetics 10, 2593–2601.

Nübler-Jung, K., Bonitz, R., Sonnenschein, M., 1987. Cell polarity during wound healing in an insect epidermis. Development 100, 163–170.

Park, M., Moon, R.T., 2002. The planar cell-polarity gene stbm regulates cell behaviour and cell fate in vertebrate embryos. Nature Cell Biology 4, 20–25.

Rachel, R.A., Murdoch, J.N., Beermann, F., Copp, A.J., Mason, C.A., 2000. Retinal axon misrouting at the optic chiasm in mice with neural tube closure defects. Genesis 27, 32–47.

Ross, A.J., May-Simera, H., Eichers, E.R., Kai, M., Hill, J., Jagger, D.J., Leitch, C.C., Chapple, J.P., Munro, P.M., Fisher, S., Tan, P.L., Phillips, H.M., Leroux, M.R., Henderson, D.J., Murdoch, J.N., Copp, A.J., Eliot, M.M., Lupski, J.R., Kemp, D.T., Dollfus, H., Tada, M., Katsanis, N., Forge, A., Beales, P.L., 2005. Disruption of Bardet-Biedl syndrome ciliary proteins perturbs planar cell polarity in vertebrates. Nature Genetics 37 (10), 1135–1140.

Simons, M., Gloy, J., Ganner, A., Bullerkotte, A., Bashkurov, M., Kronig, C., Schermer, B., Benzing, T., Cabello, O.A., Jenny, A., Mlodzik, M., Polok, B., Driever, W., Obara, T., Walz, G., 2005. Inversin, the gene product mutated in nephronophthisis type II, functions as a molecular switch between Wnt signaling pathways. Nature Genetics 37, 537–543.

Shima, Y., Copeland, N.G., Gilbert, D.J., Jenkins, N.A., Chisaka, O., Takeichi, M., Uemura, T., 2002. Differential expression of the seven-pass transmembrane cadherin genes Celsr1-3 and distribution of the Celsr2 protein during mouse development. Dev Dyn 223, 321–332.

Strong, L.C., Hollander, W.F., 1949. Hereditary *loop-tail* in the house mouse. Journal of Hereditary 40, 329–334.

Taylor, J., Abramova, N., Charlton, J., Adler, P.N., 1998. Van Gogh: a new *Drosophila* tissue polarity gene. Genetics 150, 199–210.

Theisen, H., Purcell, J., Bennett, M., Kansagara, D., Syed, A., Marsh, J.L., 1994. Dishevelled is required during wingless signaling to establish both cell polarity and cell identity. Development 120, 347–360.

Tissir, F., Goffinet, A.M., 2006. Expression of planar cell polarity genes during development of the mouse CNS. European Journal of Neuroscience 23, 597–607.

Torban, E., Kor, C., Gros, P., 2004a. Van Gogh-like2 (*Strabismus*) and its role in planar cell polarity and convergent extension in vertebrates. Trends Genetics 20, 570–577.

Torban, E., Wang, H.J., Groulx, N., Gros, P., 2004b. Independent mutations in mouse Vangl2 that cause neural tube defects in looptail mice impair interaction with members of the dishevelled family. Journal Biological Chemistry 279, 52703–52713.

Tree, D.R.P., Shulman, J.M., Rousset, R., Scott, M.P., Gubb, D., Axelrod, J.D., 2002. Prickle mediates feedback amplification to generate asymmetric planar cell polarity signaling. Cell 109, 371–381.

Usui, T., Shima, Y., Shimada, Y., Hirano, S., Burgess, R.W., Schwarz, T.L., Takeichi, M., Uemura, T., 1999. Flamingo, a seven-pass

transmembrane cadherin, regulates planar cell polarity under the control of Frizzled. Cell 98, 585–595.

Wallingford, J.B., Harland, R.M., 2002. Neural tube closure requires Dishevelled-dependent convergent extension of the midline. Development 129, 5815–5825.

Wallingford, J.B., Rowning, B.A., Vogeli, K.M., Rothbacher, U., Fraser, S.E., Harland, R.M., 2000. Dishevelled controls cell polarity during *Xenopus* gastrulation. Nature 405, 81–85.

Wang, Y., Guo, N., Nathans, J., 2006a. The role of Frizzled3 and Frizzled6 in neural tube closure and in the planar polarity of inner-ear sensory hair cells. Journal of Neuroscience 26, 2147–2156.

Wang, J., Hamblet, N.S., Mark, S., Dickinson, M.E., Brinkman, B.C., Segil, N., Fraser, S.E., Chen, P., Wallingford, J.B., Wynshaw-Boris, A., 2006b. *Dishevelled* genes mediate a conserved mammalian PCP pathway to regulate convergent extension during neurulation. Development 133 (9), 1767–1778.

Wilson, D.B., 1982. Cerebrovascular pathogenesis in the telencephalon of the loop-tail mouse: a transmission electron-microscopic study. Acta Neuropathologica (Berl) 58, 177–182.

Wolff, T., Rubin, G.M., 1998. *Strabismus*, a novel gene that regulates tissue polarity and cell fate decisions in *Drosophila*. Development 125, 1149–1159.